C. R. Physique 14 (2013) 221–227

Contents lists available at SciVerse ScienceDirect

Comptes Rendus Physique

www.sciencedirect.com

Crystal growth / Croissance cristalline

Self-organized and self-catalyst growth of semiconductor and metal wires by vapour phase epitaxy: GaN rods versus Cu whiskers

Croissance auto-organisée et auto-catalysée de fils de semiconducteurs et de métaux : Tiges de GaN par rapport aux filaments de Cu

Joël Eymery [a,*], Xiaojun Chen [a], Christophe Durand [a], Matthias Kolb [b], Gunther Richter [b]

[a] *Équipe mixte CEA–CNRS–UJF "Nanophysique et semiconducteurs", SP2M, UMR-E CEA/UJF-Grenoble 1, INAC, 38054 Grenoble, France*
[b] *Max Planck Institute for Intelligent Systems, Heisenbergstrasse 3, 70569 Stuttgart, Germany*

ARTICLE INFO

Article history:
Available online 19 February 2013

Keywords:
Crystalline growth
Wires
Mechanisms
Vapour phase
GaN
Cu

Mots-clés :
Croissance cristalline
Fils
Mécanismes
Phase vapeur
GaN
Cu

ABSTRACT

Wires represent a new class of nanostructures that offer unprecedented freedom in materials design and new physical properties. Amongst the very different growth mechanisms reported in literature, the vapour-phase growth of self-catalyzed wires has the advantages of simplicity and rapidity with a low level of contaminants. The elaborations of semiconducting and metallic wires are usually considered as very distinct fields and no significant analogies have been noticed yet. This paper illustrates significant similarities of the mechanisms involved in the GaN and Cu wire growths that highlight firstly the role of the substrate surface preparation (with the deposition of an intermediate layer on the substrate surface impacting the nucleation seeds) and secondly the role of the different diffusion paths contributing to the one-dimensional growth in particular the influence of the surrounding gas phase and respective diffusion lengths on the substrate surface and wire sidewall. Experimental data describing the evolution of the wire diameter and length as a function of the growth time are quantitatively analyzed to evidence different growth regimes.

RÉSUMÉ

Les nanofils représentent une nouvelle classe de matériaux qui offrent des possibilités nouvelles en termes de design et de propriétés physiques. Parmi les différents mécanismes de croissance rapportés dans la littérature, la croissance en phase vapeur de fils auto-catalysés présente l'avantage d'être simple et rapide, tout en assurant un faible niveau de contamination chimique. Les procédés d'élaboration des fils de semiconducteurs et de métaux sont en général considérés comme bien distincts et peu d'analogies ont été rapportées jusqu'à présent. Cet article illustre des similarités notables entre les mécanismes de croissance de fils de GaN et de Cu, qui mettent en évidence, premièrement, le rôle de la préparation de surface (avec le dépôt d'une couche intermédiaire sur le substrat qui impacte directement la nucléation des fils) et, deuxièmement, celui des différents chemins de diffusion, qui contribuent à la croissance unidimensionnelle, en particulier l'influence de la phase gazeuse environnante et des longueurs de diffusion sur la surface du substrat et sur les facettes de fils. Les données expérimentales décrivant l'évolution du diamètre et de la

* Corresponding author.
E-mail address: joel.eymery@cea.fr (J. Eymery).

1631-0705/$ – see front matter
http://dx.doi.org/10.1016/j.crhy.2012.10.009

longueur des fils en fonction du temps de croissance sont analysées quantitativement pour mettre en évidence différents régimes de croissance.

1. Introduction

Semiconducting nanowires have demonstrated potential uses in a variety of electronic and optical devices [1,2] including transistors, photovoltaics, sensors and piezoelectric generators by using composition and bandgap engineering with radial and longitudinal heterostructures. Several techniques such as metalorganic vapour phase epitaxy (MOVPE) and molecular beam epitaxy (MBE) can process such complex heterostructures and guarantee a very good control of crystallinity (single crystal) and low chemical contamination. More recently, metallic nanowhiskers have attracted large interests for example for their magnetic [3], electrical [4] and mechanical [5] properties. They can be grown by physical vapour deposition (PVD) under ultra-high vacuum with also a very high quality. Such semiconducting and metallic materials share exceptional structural properties with hair-like geometries and large length/diameter ratio although they are named differently for historical reasons: wires, columns, rods and whiskers (with the *nano* prefix for smaller diameters).

This article will enlighten the growth of self-organized and self-catalyst semiconductor and metal wires by vapour phase epitaxy taking the example of GaN rods and Cu whiskers. The self-organization provides an efficient way to get wires without preliminary surface patterning of the substrate and the lack of catalyst prevents the incorporation of chemical elements that can be detrimental to the physical properties (for example light emission in gallium nitride compounds). Note that this last point is less important in arsenide, phosphide and antimonide semiconductor compounds for which the Au catalyst used in the vapour–liquid–solid (VLS) mechanism [6,7] does not seem to influence significantly the properties of these nanowires. This paper will stress the similarities between GaN rods and Cu whiskers by analysing the experimental data describing the evolution of the wire diameter and length as a function of the growth time. The different regimes will be evidenced as well as the diffusion paths contributing to the one-dimensional growth by using the Ruth and Hirth model [8].

2. Experimental methods

2.1. MOCVD growth of GaN

The MOVPE growth of self-assembled and self-catalyzed GaN wires is performed on *c*-plane sapphire substrates in a 3×2 inch closed-coupled showerhead (CCS) reactor. This method does not require ex situ preparations of the substrate before the growth. It is based on the deposition of a thin SiN_x layer that covers the surface and plays the role of a selective layer with respect to the GaN growth [9]. It provides a robust and rapid technique ensuring a low level of contaminants convenient for industrial optoelectronic and power applications. As described in details in Ref. [10], sapphire cleaned under H_2 at high temperature is annealed under ammonia to promote the formation of an Al(O)N layer (~ 1.5 nm thick measured by X-ray reflectivity) before the deposition of a thin SiN_x layer (~ 2 nm thick) using silane and ammonia. Another ammonia annealing allows stabilizing the stoichiometry and probably favours the formation of thinnest areas or composition fluctuations that can be pierced by further deposition. The importance of these two steps of surface preparation has to be enlightened. The formation of the Al(O)N layer will define the GaN growth polarity [11]. Indeed, GaN is a pyroelectric material (non-centrosymmetric) having the wurtzite structure and it has been demonstrated that the substrate surface polarity allows controlling both the shape and the polarity of the (nano)structures: growths on *c*-sapphire and freestanding GaN substrates evidenced that N-polar oriented surface (i.e. the $-c$-axis of GaN [12]) leads to wire shape, whereas Ga-polar one leads to pyramidal shapes [13]. These features are usually summarized by drawing the kinetic Wulff-plot diagram, i.e. the growth rate as a function of the crystal growth direction for different GaN growth conditions (see Refs. [14–16]). The intermediate layer has to be adapted to the substrate to perform this substrate-polarity control e.g. an AlN layer can be deposited first on silicon (111) substrate to get similar GaN rods [17]. Its thickness has to be adjusted to support an epitaxial relationship between the objects and the substrate. In our case, the SiN_x layer prevents the nucleation and growth on covered areas between wires [18]. SiN_x and SiO_x [19] are used in selective-area growth to tailor the position and sometimes the composition of the depositions. Thick patterned masks with holes adjusted in size and density can define the lateral extension of the growth and are generally realized in a preprocessing step. In our method, the small thickness of SiN_x allows the self-organized formation of GaN seeds in epitaxy with the substrate. These seeds will then determine the size and density of the wires.

Within our approach, a high Si-dopant concentration (added by a silane flow in a majority N_2 carrier gas) and a small V/III molar ratio (ammonia to trimethylgallium) favour the vertical wire growth [10]. The experimental conditions (pressure, temperature, GaN nucleation time to form the seeds,...) are optimized to produce $-c$-oriented wires with smooth lateral $\{1\ \bar{1}\ 0\ 0\}$ m-plane facets in epitaxy with the *c*-plane sapphire substrate. A scanning electron microscopy (SEM) view of a typical growth is shown in Fig. 1(a). By adjusting the growth parameters, this method provides wires with 0.3–2 µm average diameter and quite low density in the 10^7–10^8 cm^{-2} range (see Figs. 1(b) and (c)). Note that these dimensions are well suited for optical applications and physical studies. The main advantage of the CCS reactor comes from the reproducibility and homogeneity of the process on the wafer scale. The wire epitaxial relationships on sapphire – determined by grazing incidence X-ray and electron diffraction – are equivalent to 2D layers: $[1\ \bar{1}\ 0\ 0]_{GaN}//[1\ \bar{2}\ 1\ 0]_{Al203}$ and

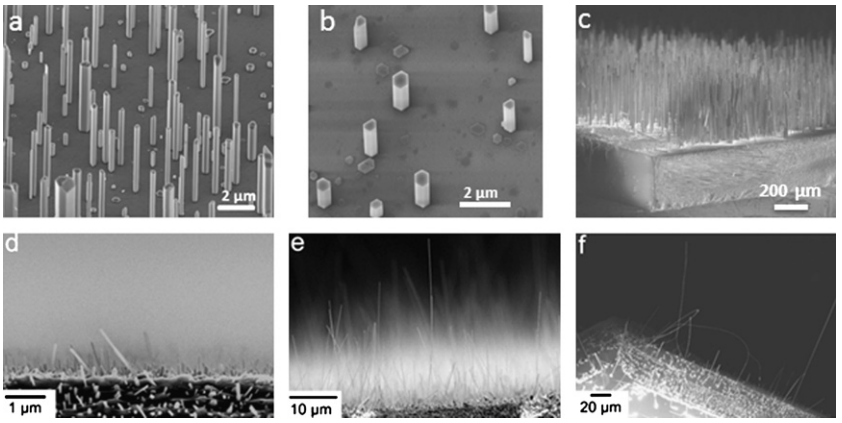

Fig. 1. (a–c) Scanning electron microscopy images of GaN rods obtained by MOCVD for different growth conditions and times. Diameter is controlled by the nucleation step and length by the time. (a) corresponds to a point of Fig. 3, (b) and (c) show example of short and long wires. (d–f) Cu nanowhiskers grown by PVD on Si(111) surfaces for different growth temperatures and times. (d) and (e) are grown at 680 °C for 5 min and 2 h respectively; (f) shows extra high aspect ratio nanowires.

$[0\ 0\ 0\ \bar{1}]_{GaN}//[0\ 0\ 0\ 1]_{Al2O3}$ with twist and tilt disorientations less than half of a degree. Transmission electron microscopy studies have shown that the wires are single crystalline and have no extended defects along the length except misfit dislocations close to the substrate interface. Threading dislocations are bent to the wire sidewall surface along a distance of the order of magnitude of the diameter [20,21]. Some anti-phase boundary separating $+c$ and $-c$ crystal orientations have been observed in self-organized wires and in guided growth close to the holes of the patterned mask [20] stressing again the importance of surface preparation and polarity control. More generally, other works have reported the formation of GaN wires by MOVPE using different experimental variants such as a pulsed injection of the precursors [21], N_2/H_2 carrier gas mixture [22–24] and very small precursor flows to be closer to thermodynamic equilibrium [25]. The main morphological differences between these growths lie in the facet orientations of the wires and polarities: in our case, the top of the wires corresponds to an almost flat $-c$-plane, whereas in other growth conditions $[1\ 0\ \bar{1}\ \bar{1}]$ and $[1\ 0\ \bar{1}\ \bar{2}]$ semipolar facets can be observed [22]. Note that a change of the growth conditions will strongly influence the surface properties of the wires: surface energies, diffusions properties, sticking coefficients,... that must be taken into account in the quantitative modelling of the growth. This constitutes the richness, but also the difficulties of the MOVPE approach compared to the MBE technique having a more limited number of parameters to play with.

2.2. PVD growth of Cu

The essential mechanism in the fabrication route for macroscopic whiskers is the condensation of metal vapour on an appropriate substrate [26]. In our synthesis method physical vapour deposition is carried out under different vacuum conditions (see experimental conditions in Ref. [5]).

Si(111) single crystals ($2 \times 10\ mm^2$) substrates are cleaned in acetone and ethanol, and subsequently introduced into a high vacuum (HV) system (base pressure 5×10^{-7} mbar). The Si wafers is plasma etched (100 W, 90 s) and then covered by a carbon layer by magnetron sputtering with a typical layer thickness of 30 nm (100 W, 492 s). The etching and C-deposition steps are carried out at room temperature. The C-coated substrate is removed from the HV system to ambient. Subsequently, it is reintroduced to vacuum conditions and transferred into an ultra-high vacuum (UHV) molecular beam epitaxy (MBE) system (base pressure $< 5 \times 10^{-10}$ mbar). Cu is deposited on the substrates at elevated substrate temperatures ($\sim 1300\,°C$). The Cu deposition rate is measured with a quartz balance and kept constant at 0.05 $nm\,s^{-1}$ for all experiments. The incidence angle of the metal vapour is 45° relative to the surface normal and the specimen plate of the MBE system can be rotated under the metal vapour beam; the rotation axis is parallel to the substrate normal. The copper is evaporated from an effusion cell. The (111) substrates have been coated for 5, 15, 30, 60 and 120 min respectively.

Microstructure characterization of the nanowires is mainly carried out by electron microscopy revealing a defect-free bulk and surface crystal structure [5,27]. No dislocations, stacking faults, or grain boundaries were detected. The growth direction is generally along the ⟨110⟩ crystallographic direction of the face centred cubic lattice and the nanowire surface is formed by the low indexed {111} and {100} crystallographic planes. The overall geometry is dominated by energy minimization (in particular the surface energy) and resembles the standard equilibrium Wulff shape. It was not possible to detect impurities from the growth process on the surface or in the bulk of the nanowires. Tensile and bending tests have been performed to study the mechanical properties of these whiskers and show flow and yield stresses close to the theoretical limits [5].

The measurements of the length and the diameter of the whiskers were carried out by SEM. Since this technique gives a 2-dimensional projection of a 3-dimensional microstructure it is difficult to measure accurately the length of inclined whiskers. Therefore the stripes were installed in such a way, that substrate surface normal was perpendicular to the electron

Table 1
Comparison of GaN rods and Cu whiskers growth.

Step	GaN rods	Cu whiskers
Surface preparation	H_2 cleaning of sapphire. Nitridation to get an Al(O)N layer.	Cathodic etching (Ar-plasma) of Si-wafer.
Deposition of a selective growth layer	SiN_x deposition by MOVPE using silane and ammonia. Its thickness is saturated to a low value (~ 2 nm) and the layer is stabilized under NH_3.	C-layer deposited by magnetron sputtering (~ 30 nm): non-wetting layer for Cu.
Seed nucleation	GaN seeds with flat surface and controlled diameter initiate the rod growth (in epitaxy with the substrate).	Holes in the C-layer act as nucleation sites. No well-defined epitaxial relationship between the substrate and the metal.
One-dimensional growth	MOVPE under majority N_2 carrier gas and a low V/III ratio. Silane addition.	Low saturation PVD (thermal evaporation) under vacuum.

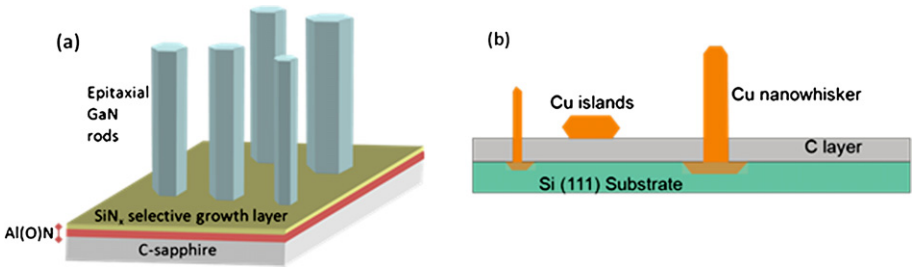

Fig. 2. Sketch of (a) GaN rods on *c*-sapphire, (b) Cu whiskers on (111) silicon.

beam. Numerous whiskers per single substrate were examined in terms of length and diameter. In all cases, only the longest whiskers were considered for comparing the experiment with the growth model.

3. Results

3.1. Discussion of the similarities between these growths

The summary of the main experimental growth procedures is given in Table 1 and schematized in Fig. 2. It shows that GaN rods and Cu whiskers are obtained with four very similar basic steps: (i) The surface preparation allows the chemical cleaning of the surface and the polarity determination, mandatory to drive the correct epitaxy of polar GaN; (ii) The selective growth layer prevents the growth on the substrate surface except in spontaneously formed hole by using materials that do not allow the seed formation or the wetting of the materials; (iii) The seed nucleation step defines the size of the wire. This step is presently more controlled for GaN materials, but Cu whiskers growth orientation and diameter could be probably improved in the future by using patterned surfaces; (iv) The specific growth parameters are chosen to favour the one-dimensional growth. A low saturation in the gas phase is used for both techniques: the ammonia flow is largely reduced with respect to planar layers (to get a low V/III molar ratio) and the thermal evaporation of Cu provides a very small quantity of materials. Silane is added in GaN wire growth and changes probably the surface properties to decrease sidewall energies with respect to $-c$-planes.

The structural quality of the wires is very good: single wires can be obtained with almost no measurable extended defects and the chemical purity of the materials can be very high: GaN rods can be n- and p-doped with Si and Mg and the Cu whiskers purity is mainly limited by the charge quality. Finally, the surface of the wires does not have thick "passivation layers" observed for example in oxide-assisted wire growth [28] that can be detrimental to further use in physical measurements or in device applications.

3.2. Kinetics of the GaN wires and Cu whiskers growths

3.2.1. Gallium nitride

It has been first checked that rods are grown in the mass-transport regime of the MOVPE: for a variation of the growth temperature between 850 and 1000 °C, the total amount of deposited material for a given growth time (t) remains constant [29]. Chemical reactions are therefore not limited by the kinetic or thermodynamic considerations, which can be very complex due to the precursor gas-phase reactivity [30–32]. The average length (l) and diameter (D) at a given growth time (t) can be determined as well as their distributions from SEM image analysis. As an example, the top view analysis of the sample shown in Fig. 1(a) gives $D \sim 400 \pm 100$ nm. The larger wires result from the coalescence of neighbouring wires and are not taken into account in the statistical analysis.

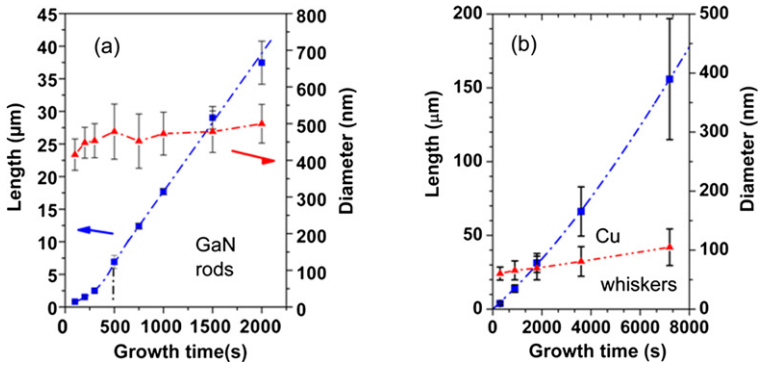

Fig. 3. Measurements of the wire length l and diameter as a function of the growth time t. The blue dash-dotted line shows fits of the $l(t)$ curves with the Ruth and Hirth model [8]. The parameter values (see text) for (a) MOVPE GaN are: $V = 18.5$ nm/s (effective linear growth rate), $I = 4$ nm/s (impingement rate at the top of the wire), $\beta = 0.1$ (substrate–wire exchange rate), $\lambda = 7.5$ μm (sidewall average diffusion length) and for (b) PVD Cu: $V = 21.7$ nm/s, $I = 1$ nm/s, $\beta = 0.5$, $\lambda = 257.3$ μm. (For interpretation of the references to colour in this figure legend, the reader is referred to the web version of this article.)

Fig. 3(a) shows the evolution of $l(t)$ and $D(t)$ at fixed standard growth conditions $T \sim 1000\,^{\circ}\mathrm{C}$, V/III ~ 20 under silane flow and majority N_2 carrier gas (see supplementary details in [10]). $l(t)$ is increasing sublinearly at the beginning of the growth to reach a linear behaviour after about $t_{\mathrm{lin.}} = 500$ s. Interestingly, $D(t)$ is almost constant for this growth-time range and no tapering effect is observed as it may be the case for catalyst-assisted growth. On the contrary, D is sightly enlarged as a function on the length. As an example, a diameter of 0.5 μm at the bottom of a 16.5 μm long wire is increased by 1.1% at the top. Moreover, it must be noted that no nucleation delay has been observed within this growth condition as it is usually the case in MBE growth. These measurements indicate a large ratio of the longitudinal to radial growth rate (i.e. between $-c$ and m directions) imposed by growth conditions and crystal polarities (the ratio being 85 for the last example). As it is shown by the error bars, the distribution of $l(t)$ is increasing with time, but this point will not be detailed in this paper. The fast average longitudinal growth rate (for time larger than $t_{\mathrm{lin.}}$) has been varied between 50 and 130 μm/h by changing flows and pressure conditions (see Fig. 1(c)). It allows growing very long wires (> 500 μm) of enlarged diameter (> 2 μm) on the full wafer in less than 4 h. The features of these very long wires must be analyzed probably more carefully and only wires having moderate length (less than 50 μm) will be considered in this paper.

3.2.2. Copper

As shown in Figs. 1(d) and (f) obtained for 5 min and 2 h growth times, most of the whiskers do not grow perpendicularly to the substrate surface. From these projected views, it is impossible to determine the angular distribution of standing whiskers, which is certainly non-random. Moreover, some islands (probably of Cu) are observed on the substrate; their sizes indicate a much lower growth rate than the whiskers. The whiskers grow in length as a function of deposition time and can reach length larger than 100 μm (see Fig. 1(f)) and at the same time a diameter thickening can be also measured.

The $l(t)$ curve is shown in Fig. 3(b) for a substrate temperature of 680 °C. One can clearly observe that the data points do not suggest a straight line for describing the growth. An asymptotic (linear) regime of the growth is not reached indicating a rather long diffusion length. In parallel, the diameter D varies almost linearly with the deposition time. The maximum length achieved after 2 h growth is $l = 150 \pm 41$ μm for $D = 100 \pm 31$ nm average diameter. This gives high aspect ratios of 1500.

3.3. Analysis with the Ruth and Hirth model

The wire length increase as a function of the growth time has been analyzed quantitatively to study further the growth mechanisms (see Fig. 3). Three main mechanisms can be proposed to explain the materials incorporation into the wires. Two contributions come from a gas phase collection with direct impingement from the top facet and upward flow coming from sidewall facet diffusion. The third pathway corresponds to the flow coming from the neighbourhood substrate surface of the wires. These three terms have been considered by Ruth and Hirth [8] and incorporated in a model considering a fixed value of the wire diameter ($D = 2R$). Within this model, the time t is expressed as a function of the length l by the following equation:

$$t = \frac{V\lambda}{\sqrt{2}(V^2 - I^2)} \mathrm{Log}\left[\frac{(\beta + \frac{I}{V})\cosh(\frac{\sqrt{2}l}{\lambda}) + (1 + \frac{\beta I}{V})\sinh(\frac{\sqrt{2}l}{\lambda})}{\beta + \frac{I}{V}}\right] - \frac{Il}{V^2 - I^2} \tag{1}$$

where $\lambda = \sqrt{2D/\omega}$ is the average facet diffusion length given by the Einstein relation (D is the surface diffusion coefficient and $1/\omega$ is the adatom stay time prior to evaporation), V is a linear-growth rate corresponding to the limiting case $\lambda \gg R$, i.e. when the direct impingement flux at the top of the wire I can be neglected. Finally, β defines the substrate-wire

exchange rate ($\beta < 1$ corresponds to a low exchange rate). The value of this parameter can be directly estimated from the shape of the $l(t)$ curve at small t.

As shown in Fig. 3, the $l(t)$ curves are well modelled for both GaN and Cu wires by the sets of values given in the figure captions.

For GaN wires, the low β value (~ 0.1) confirms the small substrate–wire exchange rate imposed by the SiN_x layer preventing any growth (and species sticking). It also shows the predominance of the gas phase incorporation mechanisms. The comparison of V and I values (18.5 and 4 nm/s respectively) shows that the facet diffusion term plays a major role to explain the high total growth rate. The mechanism driving the direct incorporation at the top of the wire (related to I) is still not explained at this time. The presence of a Ga droplet at the top of the wire – during the growth – cannot be directly checked because it may be removed by the cooling procedure and the calculations of surface energies and diffusion barriers are difficult to perform due to the influence of silicon incorporation. Finally, the value of the average diffusion length ($\lambda = 7.5$ μm) along the facets agrees with the limit between the early stage of the growth and the linear regime (see dash-dotted line in Fig. 3(a)) where the diffusion flow has reached a steady state regime. This value is consistent with standard GaN MOVPE growth.

For Cu whiskers, calculations using Ruth and Hirth's model are carried out using typical experimental diameters of the whiskers in the 50–100 nm range. The value of β (~ 0.5) agrees well with expectations from experiment. As in the case of GaN, the value of V (21.7 nm/s) is much larger than the I value (1 nm/s). Therefore, similar conclusions can be drawn concerning the importance of facet diffusion on the growth mechanism, in agreement with the very large Cu sidewall diffusion length estimated from this model (~ 200 μm).

4. Application to other systems

The influence of the selective growth layer has been reported for other self-catalyst semiconductor systems such as InAs grown by MOVPE on $GaP(111)_B$ and $Si(111)$ using a thin SiO_x layer [33] and GaAs grown by MBE on $GaAs(111)_B$ with SiO_2 [34]. For this last example, it is possible to keep the Ga catalyst at the top of the nanowire after the cooling process evidencing a clear self-catalyst mechanism with a liquid droplet during the growth; moreover the larger initial SiO_2 layer thickness allows evidencing the formation of pinholes and craters playing a role in the nucleation process. The substrate–wire adatom exchange mechanisms leading to nonlinear growth rates has been measured for the Au-catalyst growth of InAs nanowires on $InAs(111)_B$ surface [35]. The value of β can be changed from 0 to 2.5 depending on the V/III molar ratio: an increase of the trimethylindium flow rate gives a larger substrate contribution to the growth and a larger β value.

Up to now, the Ruth and Hirth model has not been applied to the modelling of core/shell heterostructures (for example AlGaN/GaN or InGaN/GaN multiple quantum wells grown around wires [36]) and to patterned growth allowing the wire positioning and the decrease of size fluctuations. Such extensions should be considered by adding different diffusion lengths and capture regions.

Applying the C-mediated PVD growth process on other face centred cubic metals results also in growth of whiskers. Especially Ag and Au follow the same trends as observed in Cu nanowhisker growth. Firstly, defects in the C layer act as nucleation site. Secondly, the surface diffusion of the metal adatoms to the whisker root contributes, at least in the early stages of growth, to the lengthening of the nanostructure. Because of this contribution, the quality and the microstructure of the C layer plays an important role on the nanowhisker formation and growth. A short summary on other metals which form nanowhiskers is given in Ref. [27].

5. Conclusion

This article pointed out strong similarities between the vapour phase growths of self-organized and self-catalyst semiconductor and metal wires. A comparison of the growth mechanisms of GaN rods and Cu whiskers has been performed. These growths occur in the small substrate–wire exchange regime imposed by the substrate preparation and are mainly driven by the gas phase incorporation coming from the sidewall diffusion and from direct impingement at the top of the wire. The Ruth and Hirth model [8] is well suited to analyse the evolution of the length of the wire as a function of time and gives quantitative values to estimate the weight of these different contributions. The atomistic mechanism of adatom incorporation is still not completely understood and should be investigated in more details.

The integration of these wire-like objects is of interest both for magnetic, electric and optoelectronic devices by simplifying contacting and doping issues. As an example, planar gallium nitride (GaN) compound heterostructures are nowadays used in the visible optoelectronics to obtain blue and white light sources and in the ultra-violet range for detection or water disinfection. In this context, the wire geometry provides several important advantages. The light extraction efficiency can be increased due to a larger free surface area and specific design. The structural quality and optical properties are much less affected by the lattice mismatch with the substrate than equivalent planar layers, and heterostructures can benefit from the elastic relaxation properties at free surface edges to relieve the strain. Single-wire light-emitting diodes and detectors based on GaN wires containing both polar and non-polar InGaN/GaN quantum wells have already demonstrated the general interest of these templates [37,38].

Metal nanowhiskers have the prospect to combine the possibilities and functionality of semiconductors wires with the inherent strength and stress resistance of metals. Since it is already proven that the theoretical strength limit is easily

achieved for Cu (and Au) nanostructures due to their defect and flaw free microstructure, it is imaginable that the electric properties of such structures are also quite unique. Metal nanowhiskers might be integrated as interconnects into devices with active semiconductor nanostructures to form novel devices. An alternative for optical properties would be to utilize surface plasmons for light emittance.

Acknowledgements

The authors thank J. Dussaud for technical support. X.J. Chen acknowledges financial support from the foundation "Nanosciences aux limites de la nanoélectronique". The work was partly funded by the French Agence nationale de la recherche MECANIX ANR-11-BS10-01401.

References

[1] C. Thelander, et al., Nanowire one-dimensional electronics, Mater. Today 9 (10) (2006) 28–35.
[2] Y. Li, F. Qian, J. Xiang, C.M. Lieber, Nanowire electronic and optoelectronic devices, Mater. Today 9 (2006) 18–27.
[3] T.M. Whitney, P.C. Searson, J.S. Jiang, C.L. Chien, Fabrication and magnetic properties of arrays of metallic nanowires, Science 261 (5126) (1993) 1316–1319.
[4] Y. Wu, J. Xiang, C. Yang, W. Lu, C.M. Lieber, Single-crystal metallic nanowires and metal/semiconductor nanowire heterostructures, Nature 430 (2004) 61–65.
[5] G. Richter, K. Hillerich, D.S. Gianola, R. Moenig, O. Kraft, C.A. Volkert, Ultrahigh strength single crystalline nanowhiskers grown by physical vapor deposition, Nano Lett. 9 (8) (2009) 3048–3052.
[6] E.I. Givargizov, Fundamental aspects of VLS growth, J. Cryst. Growth 31 (1975) 20–30.
[7] V.G. Dubrovskii, et al., Diffusion-induced growth of GaAs nanowhiskers during molecular beam epitaxy: Theory and experiment, Phys. Rev. B 71 (2005) 205325.
[8] V. Ruth, J.P. Hirth, Kinetics of diffusion-controlled whisker growth, J. Chem. Phys. 41 (10) (1964) 3139–3149.
[9] T. Akasaka, Y. Kobayashi, S. Ando, N. Kobayashi, GaN hexagonal microprisms with smooth vertical facets fabricated by selective metalorganic vapor phase epitaxy, Appl. Phys. Lett. 71 (15) (1997) 2196–2198.
[10] R. Koester, J.S. Hwang, C. Durand, D. Le Si Dang, J. Eymery, Self-assembled growth of catalyst-free GaN wires by MOVPE, Nanotechnology 21 (2010) 015602.
[11] F.D. Liu, et al., The mechanism for polarity inversion of GaN via a thin AlN layer: Direct experimental evidence, Appl. Phys. Lett. 91 (2007) 203115.
[12] Polarity in non-centrosymmetric wurtzite crystal is defined with standard notations: the bond pointing from the Ga cation to the N anion defines the polar axis *c* labelled [0001], also called Ga-polar orientation.
[13] X.J. Chen, G. Perillat-Merceroz, D. Sam-Giao, C. Durand, J. Eymery, Homoepitaxial growth of catalyst-free GaN wires on N-polar substrates, Appl. Phys. Lett. 97 (2010) 151909.
[14] Q. Sun, et al., Understanding non-polar GaN growth through kinetic Wulff plots, J. Appl. Phys. 104 (2008) 093523.
[15] D. Du, D.J. Srolovitz, M.E. Coltrin, C.C. Mitchell, Systematic prediction of kinetically limited crystal growth morphologies, Phys. Rev. Lett. 95 (2005) 155503.
[16] V. Jindal, F. Shahedipour-Sandivk, Theoretical prediction of GaN nanostructure equilibrium and nonequilibrium shapes, J. Appl. Phys. 106 (2009) 083115.
[17] A.-L. Bavencove, et al., Light emitting diodes based on GaN core/shell wires grown by MOVPE on n-type Si substrate, Electron. Lett. 47 (13) (2011) 765.
[18] M.E. Coltrin, C.C. Mitchell, Mass transport and kinetic limitations in MOCVD selective-area growth, J. Cryst. Growth 254 (2003) 35–45.
[19] Y. Kato, S. Kitamura, K. Hiramatsu, N. Sawaki, Selective growth of wurtzite GaN and $Al_xGa_{1-x}N$ on GaN/sapphire substrates by metalorganic vapor phase epitaxy, J. Cryst. Growth 144 (3–4) (1994) 133–140.
[20] X.J. Chen, et al., Wafer-scale selective area growth of GaN hexagonal prismatic nanostructures on c-sapphire substrate, J. Cryst. Growth 322 (2011) 15–22.
[21] S.D. Hersee, X.Y. Sun, X. Wang, The controlled growth of GaN nanowires, Nano Lett. 6 (2006) 1808–1811.
[22] W. Bergbauer, et al., Continuous-flux MOVPE growth of position-controlled N-face GaN nanorods and embedded InGaN quantum wells, Nanotechnology 21 (2010) 305201.
[23] Li, et al., Polarity and its influence on growth mechanism during MOVPE growth of GaN nanorods, Cryst. Growth Des. 11 (2011) 1573.
[24] C. Tessarek, S. Christiansen, Self-catalyzed, vertically aligned GaN rod-structures by metal–organic vapor phase epitaxy, Phys. Status Sol. C 9 (3–4) (2012) 596–600.
[25] X.J. Chen, B. Gayral, D. Sam-Giao, C. Bougerol, C. Durand, J. Eymery, Catalyst-free growth of high-optical quality GaN nanowires by metal–organic vapor phase epitaxy, Appl. Phys. Lett. 99 (2011) 251910.
[26] S.S. Brenner, Tensile strength of whiskers, J. Appl. Phys. 27 (12) (1956) 1484–1491.
[27] M. Schamel, et al., The filament growth of metals, Int. J. Mater. Res. 102 (7) (2011) 828–836.
[28] R.-Q. Zhang, Y. Lifshitz, S.-T. Lee, Oxide-assisted growth of semiconducting nanowires, Adv. Mater. 15 (7–8) (2003) 635–640.
[29] G.B. Stringfellow, Organometallic Vapor-Phase Epitaxy: Theory and Practice, Academic Press, London, 1999.
[30] D. Moscatelli, C. Cavallotti, Theoretical investigation of the gas-phase kinetics active during the GaN MOVPE, J. Phys. Chem. A 111 (21) (2007) 4620–4631.
[31] R.P. Parikh, R.A. Adomaitis, An overview of gallium nitride growth chemistry and its effect on reactor design: Application to a planetary radial-flow CVD system, J. Cryst. Growth 286 (2006) 259–278.
[32] A. Thon, T.F. Kuech, High temperature adduct formation of trimethylgallium and ammonia, Appl. Phys. Lett. 69 (1) (1996) 55–57.
[33] B. Mandl, et al., Growth mechanism of self-catalyzed group III–V nanowires, Nano Lett. 10 (2010) 4443–4449.
[34] A. Fontcuberta i Morral, et al., Nucleation mechanism of gallium-assisted molecular beam epitaxy growth of gallium arsenide nanowires, Appl. Phys. Lett. 92 (2008) 063112.
[35] S.A. Dayeh, E.T. Yu, D. Wang, Surface diffusion and substrate–nanowire adatom exchange in InAs nanowire growth, Nano Lett. 9 (5) (2009) 1967–1972.
[36] R. Koester, et al., M-plane core–shell InGaN/GaN multiple-quantum-wells on GaN wires for electroluminescent devices, Nano Lett. 11 (2011) 4839–4845.
[37] G. Jacopin, et al., Single-wire light-emitting diodes based on GaN wires containing both polar and non-polar InGaN/GaN quantum wells, Appl. Phys. Express 5 (2012) 014101.
[38] A. De Luna Bugallo, et al., Single-wire photodetectors based on InGaN/GaN radial quantum wells in GaN wires grown by catalyst-free metal–organic vapor phase epitaxy, Appl. Phys. Lett. 98 (2011) 233107.